Phytoplankton Calcification in a High-CO2 World
M. Debora Iglesias-Rodriguez, *et al.*
Science **320**, 336 (2008);
DOI: 10.1126/science.1154122

Phytoplankton Calcification in a High-CO_2 World

M. Debora Iglesias-Rodriguez,[1]* Paul R. Halloran,[2]* Rosalind E. M. Rickaby,[2] Ian R. Hall,[3] Elena Colmenero-Hidalgo,[3]† John R. Gittins,[1] Darryl R. H. Green,[1] Toby Tyrrell,[1] Samantha J. Gibbs,[1] Peter von Dassow,[4] Eric Rehm,[5] E. Virginia Armbrust,[5] Karin P. Boessenkool[3]

Ocean acidification in response to rising atmospheric CO_2 partial pressures is widely expected to reduce calcification by marine organisms. From the mid-Mesozoic, coccolithophores have been major calcium carbonate producers in the world's oceans, today accounting for about a third of the total marine $CaCO_3$ production. Here, we present laboratory evidence that calcification and net primary production in the coccolithophore species *Emiliania huxleyi* are significantly increased by high CO_2 partial pressures. Field evidence from the deep ocean is consistent with these laboratory conclusions, indicating that over the past 220 years there has been a 40% increase in average coccolith mass. Our findings show that coccolithophores are already responding and will probably continue to respond to rising atmospheric CO_2 partial pressures, which has important implications for biogeochemical modeling of future oceans and climate.

The climatological and ecological impacts of elevated atmospheric CO_2 partial pressures (Pco_2) are two of the most pressing environmental concerns of the present. One consequence of increasing Pco_2 in seawater is the formation of carbonic acid (H_2CO_3), which causes acidification. Carbonic acid combines with carbonate ions (CO_3^{2-}) and water molecules to form bicarbonate ions (HCO_3^-), reducing [CO_3^{2-}] and the ocean's saturation state with respect to calcite (Ω-cal), the form of calcium carbonate ($CaCO_3$) produced by coccolithophores. Elevated Pco_2 also causes an increase in [HCO_3^-], the source of carbon for calcification in coccolithophores ($Ca^{2+} + 2HCO_3^- \rightarrow CaCO_3 + CO_2 + H_2O$) (*1*). Thus, calcification is probably affected by increasing Pco_2. The precipitation from seawater of $CaCO_3$, a basic substance, lowers pH. For this reason, and because a greater fraction of dissolved inorganic carbon {DIC, the sum of HCO_3^-, CO_3^{2-}, and aqueous CO_2 [CO_2(aq)]} is present as CO_2(aq) at low pH, the formation of $CaCO_3$ in seawater stimulates an increase in the concentration of CO_2(aq) and promotes its outgassing. Consequently, a decrease in marine calcification without a concomitant decrease in organic carbon export would lead to an increased drawdown of atmospheric CO_2.

Recent evidence suggests that the increased absorption of CO_2 by the oceans, as a result of anthropogenic CO_2 release, will result in decreased calcification by corals (*2*), foraminifera (*3*), and coccolithophores (*4*–*6*). However, it has recently been shown that different coccolithophore species exhibit different calcification responses. Under increased Pco_2, a decrease in calcification has been observed for *Emiliania huxleyi* and *Gephyrocapsa oceanica* (*4*–*6*); a negligible calcification change with rising Pco_2 for *Coccolithus pelagicus* (*7*); and an increase followed by a decrease in calcification with rising Pco_2, with respect to present-day Pco_2, for *Calcidiscus leptoporus* (*7*). Most of these experiments used semicontinuous cultures, in which the carbonate system was modified by the addition of acid and/or base to control pH (*4*, *5*, *7*). Seawater pH controls the relative proportion of the carbonate species while the concentration of DIC remains constant. A more realistic representation of the ocean response to anthropogenic change is the bubbling of CO_2-enriched air through the seawater, both elevating [DIC] and decreasing pH. Recent studies with various organisms show calcification to be largely controlled by Ω-cal, rather than pH alone (*7*, *8*), and Ω-cal is controlled by both [DIC] and pH. Between the years 1800 and 2100, seawater pH is likely to fall from 8.2 to 7.8 (*9*). Achieving the required pH by CO_2 bubbling induces a greater percentage increase in [HCO_3^-] than when the same pH reduction is achieved through acid addition (which does not affect [DIC]). Therefore, to investigate calcification under future CO_2 scenarios, it is important to correctly simulate [HCO_3^-].

We designed experiments that accurately represent projections of the future carbonate system, and assessed the natural response of coccolithophores in the sedimentary record to infer these relationships over the past two centuries. Laboratory experiments tested the effect of increasing Pco_2 on calcification and other physiological parameters in the globally important coccolithophore species *E. huxleyi*. We then considered the laboratory results in the context of a field study, using sediment material from the box core RAPID 21-12-B (*10*) to examine assemblagewide changes in coccolith mass over the past ~220 years in response to anthropogenic CO_2 release.

Culture experiments. We conducted batch incubations with exponentially growing cells of the coccolithophore species *E. huxleyi* (*11*). Commercially manufactured air containing different Pco_2 was bubbled through the culture medium to adjust the Pco_2 of cultures from preindustrial levels [280 parts per million by volume (ppmv) of CO_2] up to the level predicted by one scenario for the end of the 21st century (750 ppmv of CO_2) (*12*). Our results suggest a doubling of particulate inorganic carbon (PIC) and particulate organic carbon (POC) production at 750 ppmv of CO_2. Between 280 and 490 ppmv, carbon metabolism remained broadly similar. In contrast, between 490 and 750 ppmv, both cellular PIC and POC and their production rates increased significantly (Fig. 1 and table S1). Growth rates were substantially lower at 750 ppmv of CO_2 as compared with 280, 300, and 490 ppmv of CO_2 (Fig. 1 and table S1). In parallel to the increases in POC and PIC production, analyses of particle counts and volumes (Coulter counter and flow cytometry analysis) were conducted in a subset of experiments. These analyses demonstrated that the volumes of both coccospheres (protoplast and calcium carbonate plates or coccoliths) and coccoliths increased with rising Pco_2, following a similar trend in PIC and POC (Fig. 2 and Table 1). The range of coccolith volumes is comparable to that reported in response to changing nutrient availability and salinity (*13*). Flow cytometry data indicated that the PIC increase in the medium under high Pco_2 was due to both an increase in the volume of calcite within the coccospheres and an increase in the production of detached coccoliths (Table 1). Scanning electron micrographs of cells did not reveal apparent malformation or dissolution of coccoliths under any of the experimental Pco_2 conditions (Fig. 2). Physiological changes related to increased PIC and POC production were not accompanied by alterations in the photochemical efficiency of photosystem II [the ratio of the variable-to-maximum fluorescence (Fv:Fm) ~ 0.48] (*14*), assessed using fast repetition rate fluorometry (FRRF) (*14*), indicating that cells remained "photosynthetically healthy" in all experiments (Fig. 1).

A key factor determining whether coccolithophore production represents a net source or sink of CO_2 to the atmosphere is whether the calcification-to-photosynthesis ratio is greater or less than 1.5 (*15*, *16*). The coincident increase in both PIC and POC production per cell in all the Pco_2 treatments resulted in a stable PIC:POC ratio of less than 1, although interactions with other climate-driven parameters may affect the observed trends. Our

[1]National Oceanography Centre, Southampton, University of Southampton Waterfront Campus, European Way, Southampton SO14 3ZH, UK. [2]Department of Earth Sciences, University of Oxford, Parks Road, Oxford OX1 3PR, UK. [3]School of Earth, Ocean and Planetary Sciences, Cardiff University, Main Building, Park Place, Cardiff CF10 3YE, UK. [4]Station Biologique de Roscoff, Place George Teissier, BP 74, 29682 Roscoff Cedex, France. [5]School of Oceanography, Box 357940, University of Washington, Seattle, WA 98195, USA.

*These authors contributed equally to this work.

†Present address: Departamento de Geología, Facultad de Ciencias, Universidad de Salamanca, 37008 Salamanca, Spain.

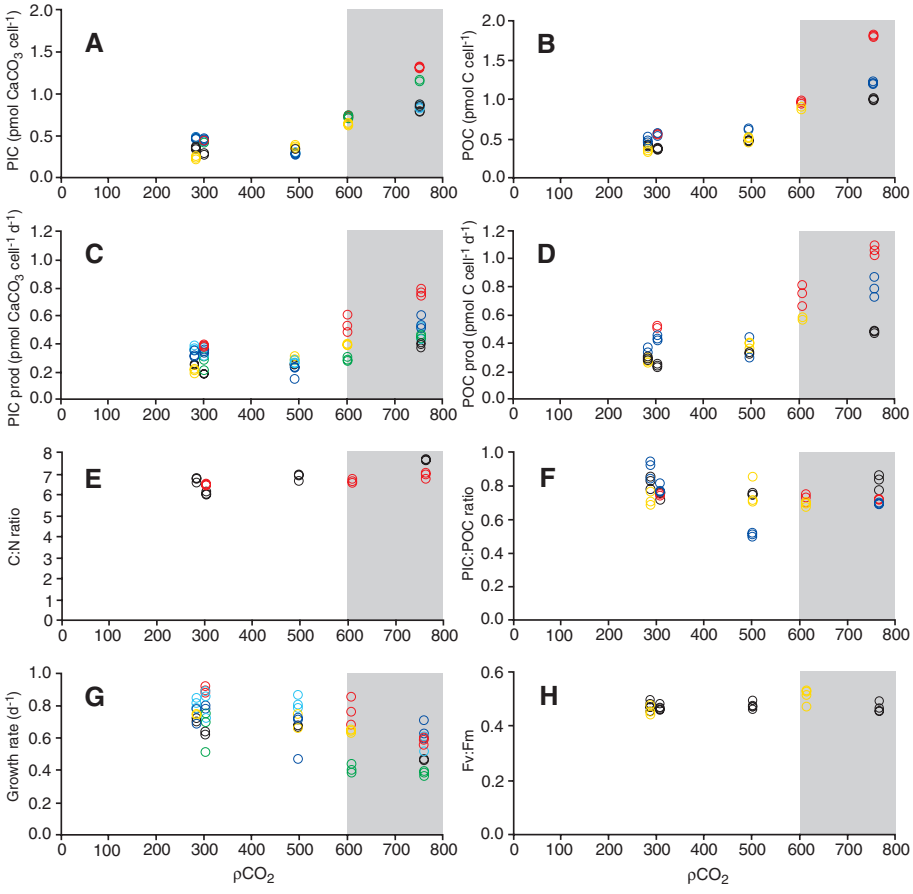

Fig. 1. Cellular PIC (**A**), POC (**B**), PIC production rates (**C**), POC production rates (**D**), C:N ratios (**E**), PIC:POC ratios (**F**), growth rates (**G**), and Fv:Fm (**H**) for *E. huxleyi* cultures under different Pco_2. Each color represents one independent experiment. Significant increases with rising Pco_2 were observed for PIC ($F_{4,16}$ = 24.14, P < 0.001), POC ($F_{4,9}$ = 10.23, P = 0.002), PIC production ($F_{4,16}$ = 5.94, P = 0.004), POC production ($F_{4,9}$ = 4.52, P = 0.028), and growth rate ($F_{4,16}$ = 3.92, P = 0.021) (table S1). Differences between the treatments of 600 and 750 ppmv of CO_2 were significant for PIC (P = 0.002) but nonsignificant (P > 0.05) for all other parameters. Cellular PIC and POC were comparable at 280, 300, and 490 ppmv of CO_2. Above 490 ppmv of CO_2, cellular PIC and POC increased significantly, by 80 and 90% respectively at 600 ppmv of CO_2, and by a further 48 and 45% respectively at 750 ppmv of CO_2. Variation in PIC and POC production rates between 280 and 490 ppmv was not significant (table S1). Between 490 and 600 ppmv of CO_2, PIC and POC production rates increased by approximately 44 and 81%, respectively, and these were approximately 30 and 18% higher at 750 than at 600 ppmv of CO_2. Growth rates were significantly lower at 750 ppmv of CO_2 as compared with 280, 300, and 490 ppmv of CO_2. Differences in PIC:POC under the different Pco_2 treatments were nonsignificant ($F_{4,9}$ = 1.22, P = 0.368) (table S1). The C:N values increased from 6.8 at 280 ppmv of CO_2 to 8.3 at 750 ppmv of CO_2. Fv:Fm values were comparable in all Pco_2 treatments. The shaded area represents putative Pco_2 during the PETM [lower-end estimates of Pco_2 were based on stomatal index and boron isotopes, data compiled in (*38*)].

results suggest that levels of Pco_2 and Ω-cal corresponding to projections for the end of this century are unlikely to affect the metabolic balance between organic carbon fixation and calcite precipitation in *E. huxleyi*.

We measured the ratios of POC to particulate organic nitrogen (C:N) to assess whether the elemental composition of the organic material was additionally affected by changing Pco_2. Variations in the elemental stoichiometry of phytoplankton are known to have an effect on trophic interactions, because the dietary value of prey items for marine zooplankton varies with the C:N ratio (*17*). Previous studies have reported changes in the elemental composition of diatoms in response to variations in Pco_2 (*18*). The C:N ratios in *E. huxleyi* increased from 6.8 to 8.3 with rising Pco_2 between 280 and 750 ppmv of CO_2 (Fig. 1). These results indicate that the Pco_2 could affect the grazing-selection pressure on phytoplankton, representing different "food" qualities. Grazing selection has many biogeochemical consequences and in particular implications for the export flux of carbon (*17*).

Our data show that Ω-cal ranged from 5.3 at 280 ppmv of CO_2 to 2.6 at 750 ppmv of CO_2, corresponding to an average total alkalinity of 2292 μeq liter^{-1} (Table 2). Ω-cal values were within the range of those for most of the upper-ocean regions, and well above 1, the threshold value below which dissolution would occur. In this pH range, less than 10% of the DIC in the medium was taken up by the proliferating cells (Table 2). Comparing these values with those in the corresponding blanks (without *E. huxleyi* cells) shows that cell physiology caused a shift in pH of less than 0.04 units in all experiments (Table 2). The pH values of the cultures incubated at 280 and 750 ppmv of CO_2 ranged between 8.1 and 7.7 (corresponding to 9.5 μM CO_2 and 25.1 μM CO_2, respectively). These changes did not affect the photosynthetic health of cells (Fig. 1), which implies our pH conditions were within the tolerance levels of *E. huxleyi*. A

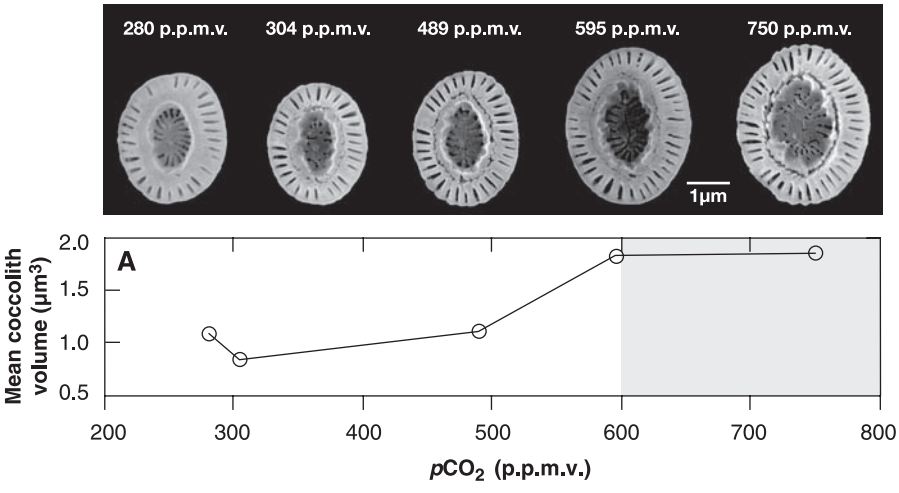

Fig. 2. Coccolith volume and $CaCO_3$ per cell. Increasing coccolith volume is closely coupled with increasing $CaCO_3$ per cell, indicating down-core measurement of coccolith mass to be representative of $CaCO_3$ production. Scanning electron microscope (SEM) images show typical coccoliths from each culture with Pco_2 values from 280 to 750 ppmv of CO_2, of where the measured volume was converted to length using the formula for a heavily calcified coccolith (*27*).

similar conclusion was reached in (*19*), where pH values within the range of those measured here did not suppress calcification. Our results are unlikely to be due to the physiological traits of a particular strain of *E. huxleyi*, because we observed the same effects on calcification and organic carbon production in another calcifying strain of *E. huxleyi* (61/12/4, Marine Biological Association, Plymouth, UK).

Down-core observations. In light of our laboratory results, which show a correlated increase in PIC and coccolith size with elevated P_{CO_2}, we investigated the response of a natural coccolithophore assemblage at high latitude to anthropogenic ocean acidification since the Industrial Revolution. We developed a method that can estimate the average mass of calcite per coccolith across multiple coccolithophore taxa (*11*). This technique was applied to material from the box core RAPID 21-12-B (57°27.09′N, 27°54.53′W), situated at 2630 m water depth in the subpolar North Atlantic. Core RAPID 21-12-B contains unprecedented open-ocean sedimentation rates of 2.3 mm $year^{-1}$ spanning the time interval from 1780 to 2004 C.E. (*10*), which allows a detailed view of coccolith formation over the Anthropocene period, the period of anthropogenic CO_2 release.

Sediment was filtered at 10 μm to obtain the coccolith fraction, excluding larger carbonate grains (*11*) (fig. S1). The mass of calcite in two subsamples at each depth was measured in triplicate, and the number of $CaCO_3$ particles between 0.63 and 10 μm [reasonably assumed to be coccoliths (*20*, *21*)] was counted nine times with an electrical resistance pulse detector (Coulter counter). Measurements were made before and after the addition of acid to account for the non-$CaCO_3$ component of the sediment. An upper detection limit of 10 μm was chosen to focus observations on particles with cohesive behavior and to avoid sampling the drift component of the sediment (*22*). This method excludes coccoliths with a diameter >10 μm. Only coccoliths of *C. pelagicus braarudii* were consistently >10 μm and were correspondingly excluded from the species counts. This approach measures the average mass of calcite per coccolith, which integrates any change in $CaCO_3$ mass due to variations in the assemblage and to intraspecies shifts in coccolith mass. To examine whether changes in species composition could account for the observed trend, coccolith assemblages were counted under a light microscope, following standard techniques for preparation by settling (*23*). No significant trend in species composition (Fig. 3) nor estimated species mass contribution (fig. S2) was observed. Dividing automated particle counts by sample weights before and after the removal of $CaCO_3$ by dissolution, and subtracting postdissolution measurements from predissolution measurements, not only rapidly provided average mass data on a large number of coccoliths (average sample counts were ~80,000 $CaCO_3$ particles), but was also sensitive to volume changes in the coccolith in any dimension.

The average mass of $CaCO_3$ per coccolith increased from 1.08×10^{-11} to 1.55×10^{-11} g between 1780 and the modern day (Fig. 4), with an accelerated increase over recent decades (fig. S3). Evidence is building that coccoliths are more resistant to dissolution than are planktonic foraminifera (*24*) and that they remain pristine when exposed to fluids in the pH range of 6 to 8 (*25*). In agreement with these observations, the absence of any down-core trend in coccolith species abundance in RAPID 21-12-B, despite the presence of taxa exhibiting a range of suscep-

Table 1. Coccosphere and coccolith volumes of *E. huxleyi* cells under different P_{CO_2} measured using a Coulter counter and flow cytometer. *t* tests of pairwise comparisons of the mean coccosphere and coccolith volumes measured by Coulter counter gave *P* values below 0.01 for all the pairwise comparisons. Side scatter (here in relative units, normalized to the side scatter of 3-μm internal bead standards) correlates strongly with the cellular calcification of *E. huxleyi* (*39*), whereas forward scatter correlates with coccosphere size. Comparison of forward-scatter volume before and after acidification indicates that the differences in volume among the different P_{CO_2} were due both to the amount of calcite and to the size of the organic protoplast. The difference between Coulter counter versus flow cytometer volume measurements may be an effect of the different ways that the volume is calculated by these two instruments (electronically versus optically). nd, not determined.

	Coulter counter		Flow cytometer		
P_{CO_2}	Average coccosphere Coulter volume (μm^3)	Average coccolith volume (μm^3)	Average coccosphere side scatter (relative to 3-μm beads) (relative units)	Coccosphere forward-scatter volume before/after acidification (μm^3)	Average number of detached coccoliths per coccosphere
280.00	55.44	1.09	3.86	115/66.1	13.2
303.79	45.95	0.84	3.84	111/57.4	10.3
489.18	65.13	1.11	3.89	123/63.6	24.2
595.09	55.23	1.84	nd	nd	nd
750.25	69.33	1.86	4.05	155/77.1	80.3

Table 2. Carbonate chemistry in *E. huxleyi* cultures corresponding to different CO_2 scenarios from preindustrial time to projections for the end of this century (*11*). For each parameter, the numbers in the first row represent average values measured in the exponential growth phase, the numbers in the second row represent the blank values at the beginning of the experiment, and the values in the third row correspond to 1 SD of three samples.

Parameter	Preindustrial	Circa 1930	2035	2060	2100
P_{CO_2} (ppmv)	280.0	303.8	489.2	595.1	750.2
	268.2	326.3	524.8	726.2	844.1
	0.3	0.2	3.5	9.2	3.0
$[CO_2]$ (μmol $liter^{-1}$)	9.5	10.2	16.4	19.9	25.1
	9.0	10.9	17.6	24.3	28.2
	0.0	0.0	0.1	0.3	0.1
$[CO_3^{-}]$ (μmol $liter^{-1}$)	222.7	215.0	157.3	112.1	108.5
	244.0	216.4	157.7	123.3	110.0
	0.3	0.0	0.8	1.4	0.4
[DIC] (μmol $liter^{-1}$)	1906.9	1923.5	2016.7	1848.1	2028.9
	1952.6	1993.2	2086.4	2136.1	2162.6
	0.7	0.6	1.0	1.1	0.2
$[HCO_3^{-}]$ (μmol $liter^{-1}$)	1674.7	1698.2	1843.0	1716.0	1895.3
	1699.6	1765.8	1911.2	1988.4	2024.4
	0.3	0.6	1.7	2.2	0.4
Ω-calc	5.34	5.16	3.77	2.69	2.60
	5.85	5.19	3.78	2.96	2.64
	0.00	0.00	0.02	0.03	0.01
pH	8.15	8.13	7.96	7.85	7.79
	8.19	8.12	7.95	7.82	7.77
	0.00	0.00	0.00	0.01	0.00
Alkalinity (μeq $liter^{-1}$)	2220.3	2224.9	2227.6	1995.9	2161.7
	2294.0	2292.8	2294.6	2288.3	2291.6
	1.2	0.6	0.3	1.3	0.4

tibilities to dissolution, indicates that our observed increase in coccolith mass cannot be accounted for by changing species compositions or dissolution effects (*26*).

The increase of ~4.5 pg in the average mass of $CaCO_3$ per coccolith since ~1960, as indicated by the smoothed least-squares curve in Fig. 4, coincides with rising atmospheric P_{CO_2} and is consistent in direction and relative magnitude with changes demonstrated here using laboratory experiments with *E. huxleyi* under future CO_2 scenarios. On average, 75% by mass of the <10-μm calcite (calculated by multiplying coccolith counts by typical coccolith volumes) at site RAPID 21-12-B constitutes coccoliths of only two taxa, *C. pelagicus pelagicus* and *Calcidiscus leptoporus,* and just 3.2% comes from *E. huxleyi* (fig. S2). Typical coccoliths of the massive *C. pelagicus pelagicus* and *Calcidiscus leptoporus* species are approximately 15 and 7 times the average pre-1960 coccolith mass, respectively (*27*), and *C. pelagicus pelagicus* alone would require a <5% increase in coccolith mass (equivalent to a ~0.25-μm diameter increase) to account for the entire observed coccolith mass change, which is well within present-day variability (*27*). Therefore, because changes in the average coccolith mass can be dominated by only a small number of heavily calcifying species, it is quite possible that the global calcification response may vary greatly with coccolithophore species assemblage in alternative oceanic regimes. However, the dominance of *C. pelagicus pelagicus* over the sedimentary calcite mass observed in this core is typical within the North Atlantic (*27–29*), and therefore our findings probably represent a regional response, the response of a basin highly sensitive to anthropogenic CO_2 production (*9*). If species other than *E. huxleyi* also exhibit a concomitant increase in PIC and POC production with rising CO_2 as demonstrated here for *E. huxleyi*, there would be no net change in this ratio with time, but we cannot quantify this ratio without a record of total organic carbon production. Nevertheless, a potential consequence of increasing calcification is a greater removal of POC from the surface waters because of increased ballast effects (*30*), although it is inconclusive whether or to what degree increased $CaCO_3$ ballast would favor a relative increase in POC export (*31*).

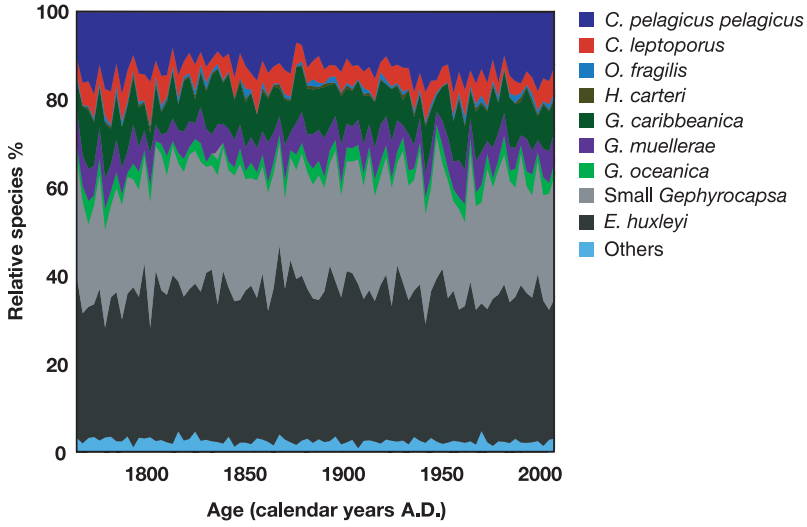

Fig. 3. Relative percentage abundance of coccoliths of each species in RAPID 21-12-B counted under a light microscope. No long-term trend in species composition was observed, indicating little or no species response to anthropogenic forcing. Stasis in the species composition, as would be expected considering the small temperature variation over this interval, implies that the core material is unaffected by dissolution (*26*), which was confirmed by SEM examination. The observed species assemblage is consistent with those published for other central subpolar Atlantic sites (*27, 29*).

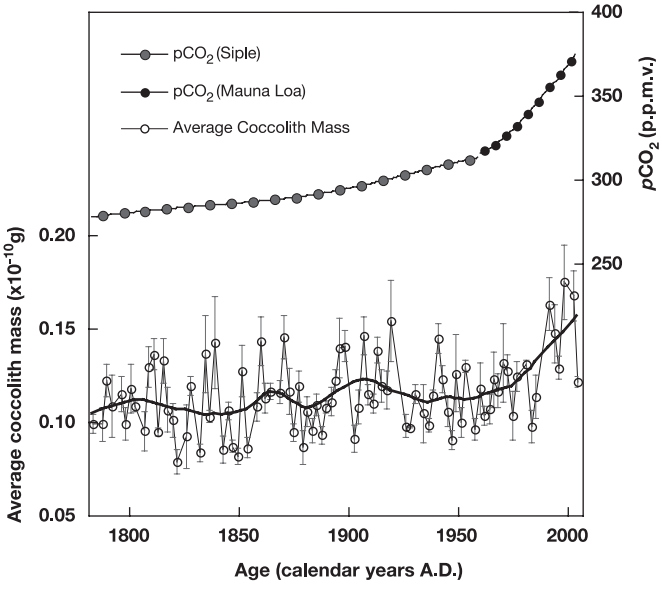

Fig. 4. Average mass of $CaCO_3$ per coccolith in core RAPID 21-12-B and atmospheric CO_2. The average mass of $CaCO_3$ per coccolith in core RAPID 21-12-B (open circles) increased from 1.08×10^{-11} to 1.55×10^{-11} g between 1780 and the modern day, with an accelerated increase over recent decades. The increase in average coccolith mass correlates with rising atmospheric P_{CO_2}, as recorded in the Siple ice core (gray circles) (*26*) and instrumentally at Mauna Loa (black circles) (*38*), every 10th and 5th data point shown, respectively. Error bars represent 1 SD as calculated from replicate analyses. Samples with a standard deviation greater than 0.05 were discarded. The smoothed curve for the average coccolith mass was calculated using a 20% locally weighted least-squares error method.

Discussion. Delving into the geological record potentially provides additional insight into coccolithophore response to elevated P_{CO_2}. Preservation of calcareous nannofossils relies on a buffering of the Ω-cal by vertical migration of the calcite compensation depth (CCD), the depth at which the rate of calcite input from surface waters equals the rate of dissolution. On time scales of >10,000 years, the CCD buffer keeps Ω-cal relatively constant (*32*); however, on shorter time scales there have been intervals in the geological past where the CCD has temporally shoaled, suggesting ocean acidification and transient decreases in carbonate saturation. The most widely studied of these intervals is the Paleocene Eocene Thermal Maximum (PETM, ~55 million years ago) (*33*). Calcareous nannofossil records suggest no obvious reduction in their abundance, shifts in distribution, or evolutionary bias attributable to ocean acidification during the PETM (*34*). The pH and P_{CO_2} reached in our culture experiments are within estimates of those indicated for the PETM (Fig. 1), and our laboratory and field results are again consistent with the lack of evidence for a change in saturation state being detrimental to coccolithophores.

Our single-species culture experiments and high-latitude assemblage records suggest that in a scenario where the P_{CO_2} in the world's oceans increases to 750 ppmv, coccolithophores will double their rate of calcification and photosynthesis (if ecosystem processes allow the survival of similar numbers of larger coccolithophore cells in the future). Given that coccolithophores are a major contributor [about 50% (*35*)] to the open-ocean carbonate pump, but a much smaller contributor [about 10% (*36*)] to the soft-tissue pump, we expect a disproportionate impact on overall community rates of calcification. Our experiments were conducted on *E. huxleyi*, which forms blooms at high latitudes that provide a snapshot of the response of *E. huxleyi* to P_{CO_2} under nutrient-replete conditions. Previous work using chemostat cultures under nutrient-limiting conditions (*37*) showed that increasing P_{CO_2} resulted in a decrease

in net calcification rate and gross community production but had no noticeable effect on the ratio of calcification to photosynthesis. Other species need to be investigated in light of the variability encountered in response to changing P_{CO_2} between coccolithophore species that are representative of low and mid-latitudes (*25*).

Future research is needed to fully constrain productivity changes over the Anthropocene period, extend our understanding of calcification changes at different latitudes and in different ocean basins, and quantify how changing ballast will affect export production. The widely held assumption that all coccolithophores will decrease their calcification under elevated P_{CO_2} needs reappraisal in the light of our laboratory and field observations that demonstrate enhanced PIC production and cell size under high P_{CO_2} conditions and the resilience of calcifying phytoplankton in the geological record (*34*). Our analyses are highly relevant to ocean biogeochemical modeling studies and underline the physiological and ecological versatility of coccolithophores and their evolutionary adaptation through changes in ocean carbonate chemistry associated with past and projected P_{CO_2} levels.

References and Notes

1. E. Paasche, *Phycologia* **49**, 503 (2002).
2. J. A. Kleypas *et al*., *Science* **284**, 118 (1999).
3. J. Bijma, H. J. Spero, D. W. Lea, B. E. Bemis, in *Use of Proxies in Paleoceanography: Examples from the South Atlantic*, G. Fischer, G. Wefer, Eds. (Springer, Berlin, 1999), pp. 489–512.
4. U. Riebesell *et al*., *Nature* **407**, 364 (2000).
5. I. Zondervan, R. E. Zeebe, B. Rost, U. Riebesell, *Global Biogeochem. Cycles* **15**, 507 (2001).
6. B. Delille *et al*., *Global Biogeochem. Cycles* **19**, GB2023, 10.1029/2004GB002318 (2005).
7. G. Langer *et al*., *Geochem. Geophys. Geosyst.* **7**, Q09006 (2006).
8. S. Trimborn, G. Langer, B. Rost, *Limnol. Oceanogr.* **52**, 2285 (2007).
9. R. A. Feely *et al*., *Science* **305**, 362 (2004).
10. K. P. Boessenkool, I. R. Hall, H. Elderfield, I. Yashayaev, *Geophys. Res. Lett.* **34**, 10.1029/2007GL030285 (2007).
11. Materials and methods are available as supporting material on *Science* Online.
12. K. Caldeira, M. E. Wickett, *Nature* **425**, 365 (2003).
13. J. Bollmann, J. O. Herrle, *Earth Planet. Sci. Lett.* **255**, 273 (2007).
14. Z. S. Kolber, O. Prasil, P. G. Falkowski, *Biochim. Biophys. Acta* **1367**, 88 (1998).
15. This "balance point" [the calcification-to-photosynthesis ratio at which a bloom has zero net impact on atmospheric CO_2 (C:P)] was calculated as having a value of about 1.5 at [DIC] = 2050 μmol kg^{-1}, [Alk] = 2300 μeq kg^{-1}, temperature = 15°C, and salinity = 35. The value of the balance point C:P ratio exhibits some variability with in situ conditions. For instance, it varies in the range 1.0 to 1.8 as in situ conditions vary in the ranges [DIC] = 2000 to 2300 μmol kg^{-1}, [Alk] = 2200 to 2400 μeq kg^{-1}, temperature = 10 to 30°C and salinity = 33 to 37. Its value will decrease by about 20% as P_{CO_2} increases from 280 ppmv to 700 ppmv (other conditions remaining constant) (*16*).
16. M. Frankignoulle, C. Canon, J.-P. Gattuso, *Limnol. Oceanogr.* **39**, 456 (1994).
17. T. R. Anderson, P. Pondaven, *Deep-Sea Res. I* **50**, 573 (2003).
18. S. Burkhardt, I. Zondevan, U. Riebesell, *Limnol. Oceanogr.* **44**, 683 (1999).
19. N. A. Nimer, M. J. Merrett, *New Phytol.* **123**, 673 (1993).
20. H. Z. Wang, I. N. McCave, *J. Geol. Soc. London* **147**, 373 (1990).
21. M. Frenz, K. H. Baumann, B. Boeckel, R. Hoppner, R. Henrich, *J. Sediment. Res.* **75**, 464 (2005).
22. I. N. McCave, I. R. Hall, *Geochem. Geophys. Geosyst.* **7**, Q10N05 (2006).
23. J. A. Flores, F. J. Sierro, *Micropaleontology* **43**, 321 (1997).
24. M. Frenz, R. Henrich, *Sedimentology* **54**, 391 (2007).
25. L. Beaufort, I. Probert, N. Buchet, *Geochem. Geophys. Geosyst.* **8**, Q09011, 10.1029/2006GC00149.
26. M. E. Hill, *Micropaleontology* **21**, 227 (1975).
27. J. R. Young, P. Ziveri, *Deep-Sea Res. II* **47**, 1679 (2000).
28. P. Ziveri, K. H. Baumann, B. Bockel, J. Bollmann, J. Young, in *Coccolithophores: From Molecular Processes to Global Impact*, H. Thierstein, J. Young, Eds. (Springer, Berlin, 2004), pp. 403–428.
29. A. McIntyre, A. W. H. Bé, *Deep-Sea Res.* **14**, 561 (1967).
30. D. Archer, E. Maier-Reimer, *Nature* **367**, 260 (1994).
31. S. Barker, J. A. Higgins, H. Elderfield, *Philos. Trans. R. Soc. London Ser. A* **361**, 1977 (2003).
32. T. Tyrrell, R. E. Zeebe, *Geochim. Cosmochim. Acta* **68**, 3521, 10.1016/j.gca.2004.02.018 (2004).
33. J. C. Zachos *et al*., *Science* **308**, 1611 (2005).
34. S. J. Gibbs, P. R. Bown, J. A. Sessa, T. J. Bralower, P. A. Wilson, *Science* **314**, 1770 (2006).
35. K. H. Baumann, H. Andruleit, B. Bockel, M. Geisen, H. Kinkel, *Palaontol. Z.* **79**, 93 (2005).
36. A. J. Poulton, T. R. Adey, W. M. Balch, P. M. Holligan, *Deep-Sea Res. II* **54**, 538 (2007).
37. A. Sciandra *et al*., *Mar. Ecol. Prog. Ser.* **261**, 111 (2003).
38. D. L. Royer, R. A. Berner, I. P. Montañez, N. J. Tabor, D. J. Beerling, *GSA Today* **14**, 10.1130/1052-5173(2004) 0142.0.CO;2 (2004).
39. C. D. Keeling, T. P. Whorf, in *Trends: A Compendium of Data on Global Change* (Carbon Dioxide Information Analysis Center, Oak Ridge National Laboratory, U.S. Department of Energy, Oak Ridge, TN, 2005).
40. J. D. L. van Bleijswik, R. S. Kempers, M. J. Veldhuis, *J. Phycol.* **30**, 230 (1994).

41. The authors acknowledge M. Hill for manufacturing the bubbling flasks, B. Alker for her assistance in PIC preparation and analysis, D. Hydes for access to the Versatile Instrument for the Determination of Titration Alkalinity instrument, R. Head for POC analysis, and R. Gibson for assistance with PIC and FRRF analysis. We thank H. Medley for laboratory assistance and J. Elliot for useful discussions. We are grateful to the master, officers, crew, and scientific party of the *RRS Charles Darwin* cruise CD159, in particular I. N. McCave and H. Elderfield. We are grateful to O. M. Schofield, P. A. Tyler, and T. Anderson for discussions on the manuscript. We thank K. Davis for assistance with graphic illustrations. This work was supported by the Royal Society research grant no. 24437 (M.D.I.-R.) and by the Betty and Gordon Moore Foundation Marine Microbiology Investigator Award (flow cytometry analysis) (E.V.A.). The field work was supported by the UK Natural Environment Research Council RAPID Program. P.R.H. acknowledges support from Natural Environment Research Council (NERC) grant no. NER/S/S/2004/12772. R.E.M.R. and I.R.H. gratefully acknowledge NERC grant no. NER/T/S/2002/00980.

Supporting Online Material

www.sciencemag.org/cgi/content/full/320/5874/336/DC1
Materials and Methods
Figs. S1 to S3
Tables S1 and S2
References

13 December 2007; accepted 3 March 2008
10.1126/science.1154122

The Global Circulation of Seasonal Influenza A (H3N2) Viruses

Colin A. Russell,[1] Terry C. Jones,[1,2,3] Ian G. Barr,[4] Nancy J. Cox,[5] Rebecca J. Garten,[5] Vicky Gregory,[6] Ian D. Gust,[4] Alan W. Hampson,[4] Alan J. Hay,[6] Aeron C. Hurt,[4] Jan C. de Jong,[2] Anne Kelso,[4] Alexander I. Klimov,[5] Tsutomu Kageyama,[7] Naomi Komadina,[4] Alan S. Lapedes,[8] Yi P. Lin,[6] Ana Mosterin,[1,3] Masatsugu Obuchi,[7] Takato Odagiri,[7] Albert D. M. E. Osterhaus,[2] Guus F. Rimmelzwaan,[2] Michael W. Shaw,[5] Eugene Skepner,[1] Klaus Stohr,[9] Masato Tashiro,[7] Ron A. M. Fouchier,[2] Derek J. Smith[1,2]*

Antigenic and genetic analysis of the hemagglutinin of ~13,000 human influenza A (H3N2) viruses from six continents during 2002–2007 revealed that there was continuous circulation in east and Southeast Asia (E-SE Asia) via a region-wide network of temporally overlapping epidemics and that epidemics in the temperate regions were seeded from this network each year. Seed strains generally first reached Oceania, North America, and Europe, and later South America. This evidence suggests that once A (H3N2) viruses leave E-SE Asia, they are unlikely to contribute to long-term viral evolution. If the trends observed during this period are an accurate representation of overall patterns of spread, then the antigenic characteristics of A (H3N2) viruses outside E-SE Asia may be forecast each year based on surveillance within E-SE Asia, with consequent improvements to vaccine strain selection.

Influenza A (H3N2) virus is currently the major cause of human influenza morbidity and mortality worldwide. On average, influenza viruses infect 5 to 15% of the global population, resulting in ~500,000 deaths annually (*1*). Despite substantial progress in many areas of influenza research, questions such as when and to what extent the virus will change antigenically, and to what extent viruses spread globally, remain unanswered. A fundamental issue behind these questions is whether epidemics are the consequence of low-level persistence of viruses from the previous epidemic or whether they are seeded from epidemics in other regions and, if so, from where (*2*–*8*).

Addressing these issues of local persistence and global spread is vitally important for designing optimal surveillance and control strategies. If epidemics were regularly seeded from an outside region and if the source region of seed strains could be identified, it may be possible to forecast which variants would appear in epidemics in seeded